SANDIA REPORT

SAND84-8238 • Unlimited Release • UC-62e

Printed October 1984

Solid Particle Receiver Experiments: Velocity Measurements

J. M. Hruby and V. P. Burolla

Prepared by
Sandia National Laboratories
Albuquerque, New Mexico 87185 and Livermore, California 94550
for the United States Department of Energy
under Contract DE-AC04-76DP00789

SF 2900-Q(6-82)

Issued by Sandia National Laboratories, operated for the United States Department of Energy by Sandia Corporation.

Printed in the United States of America
Available from
National Technical Information Service
5285 Port Royal Road
Springfield, VA 22161

NTIS price codes
Printed copy: A03
Microfiche copy: A01

SAND84-8238
Unlimited Release
Printed October 1984

SOLID PARTICLE RECEIVER EXPERIMENTS: VELOCITY MEASUREMENTS

J. M. Hruby
V. P. Burolla

Solar Components Division
Sandia National Laboratories, Livermore

ABSTRACT

Laser Doppler velocimetry and other photometric techniques are evaluated for measuring the average particle velocity in an ensemble of free-falling particles. The ability to obtain measurements in the presence of a radiant flux as high as 0.6 MW/m^2 was part of the evaluation. Optically dissimilar particles with diameters ranging from 0.1 mm to 1 mm were used in the study. Experimental results indicate that ensembles of particles do not behave as single isolated particles. The particle motion is dependent on particle volume fraction, and is quite unstable for falls greater than one meter.

CONTENTS

LIST OF ILLUSTRATIONS

SUMMARY

As part of the solid particle solar thermal central receiver technical feasibility study, a diagnostic technique to measure particle velocity in an ensemble of free-falling particles was developed. The particle diameters of interest range from 0.1 to 1 mm, and particle volume fractions are less than 0.1 percent. Because this technique must be capable of measuring particle velocity in a full scale solid particle receiver there are several requirements that must be considered. Specifically, a device measuring particle velocity will have to operate at least two meters away from the region of interest to insure that the instruments do not receive direct radiant flux or indirect radiation from heated surfaces. In addition, it must be capable of making measurements (1) on optically different types of particles, (2) in several directions, and (3) in a background of high intensity solar flux.

Several techniques were evaluated for particle velocity measurement, and laser Doppler velocimetry (LDV) was chosen as the technique to pursue. Each technique considered for particle velocity measurement is discussed herein, and a detailed discussion of LDV is included. The two techniques which proved most successful were electronic flash photography and LDV. This application of LDV is different from usual applications due to the relatively large size, irregular shape, and optical characteristics of the particles of interest. Successful measurements were completed with a simple optical arrangement.

The particle velocities measured with an electronic flash photographic technique and LDV are presented and compared. The accuracy associated with flash photography and LDV is 10 percent and 3 percent respectively. The velocities obtained from the two techniques agree well although the photographic technique is biased towards slow moving particles. Particle velocities measured in room temperature ensembles of free-falling particles are higher than the velocity of a free-falling single isolated sphere. Macroscopic curtain instability is present after approximately one meter of fall.

1. INTRODUCTION

A novel concept [1,2] for a solar thermal central receiver is currently being evaluated at Sandia National Laboratories. In this receiver, the solar insolation is absorbed directly into an ensemble or curtain of free-falling particles distributed within a cavity. This is a departure from the present solar receiver concepts which employ "fluid-in-tube" heat exchangers to absorb the solar energy. It is believed that a particle receiver can deliver higher temperature thermal energy than the current solar heat exchanger receivers which are limited to temperatures of about 550 degrees C. A conceptual design of a particle receiver is shown in Figure 1. Of primary concern in the receiver design is the time the particles spend in the solar flux, because this affects the final particle temperature. A thorough understanding of particle velocities is therefore required to predict the particle residence time, and thus the net amount of particle heating.

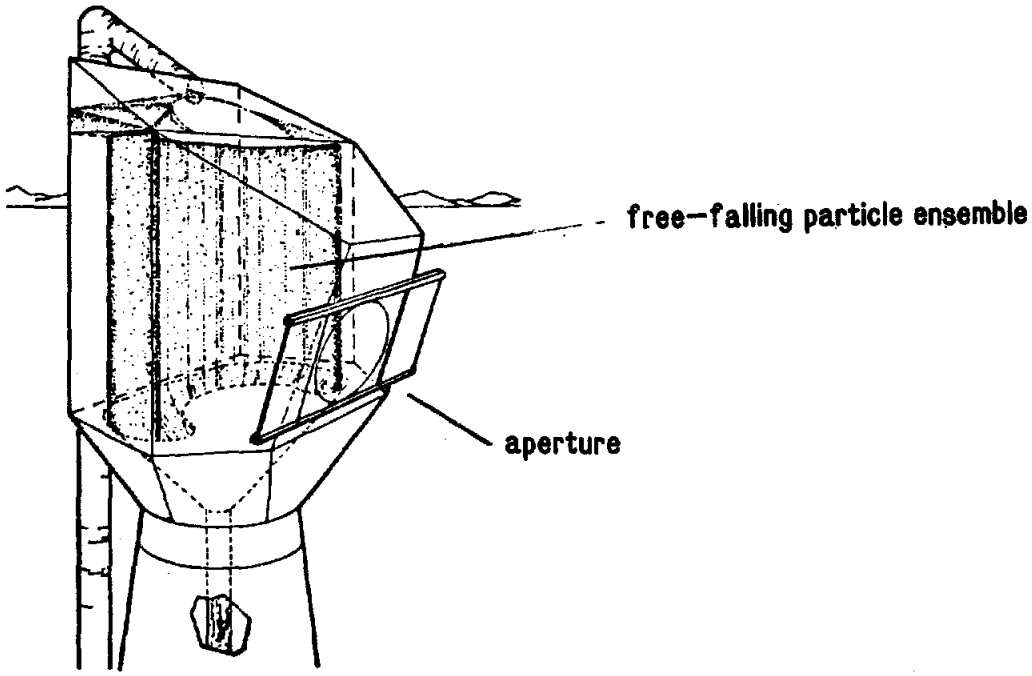

Figure 1. Conceptual design of a solid particle receiver

Much work has been reported in the literature [3] that characterizes the aerodynamic behavior of single particles falling in stagnant air. However, little information is available on suspensions of falling particles. As one would expect, each particle drags with it some envelope of surrounding air so that the air velocity is no longer zero. Modeling the action of the falling particles in a solar cavity requires an understanding of the radiative exchange as well as the motion of the air. Due to the complexity and time involved in developing analytical models to describe the flow field, an experimental program was conducted simultaneously. The experimental program provides data for use in the modeling effort and in the appraisal of the particle receiver concept.

The focus of this paper is an evaluation of flow field characterization techniques which can be used in dilute gaseous suspensions of particles. Several techniques for remote particle velocity measurement were considered, and each is described in Section 2. Laser Doppler velocimetry was chosen as the technique to pursue further, and a detailed discussion of this technique is included in Section 3. The velocity profiles by these various techniques are then presented and discussed in Section 4.

The velocity measurement program is one of three major experiments planned as part of a proof of concept program for the solid particle receiver. Another experiment involves radiating ten meters of falling particles with a bank of infrared lamps and will be discussed in detail in the second report of this series on solid particle receiver experiments. The third report of the series will discuss experiments designed to determine convective losses from falling ensembles of particles.

Experimental Apparatus

The experiments designed to observe the aerodynamic behavior of particle laden curtains were laboratory scale efforts involving no radiant flux, common grade sand (approximately 0.3 mm diameter), subscale curtains (6 mm and 12 mm thick by 150 mm wide), and drop heights of less than six meters. A photograph of the experimental apparatus is shown in Figure 2. Those flow field measurement

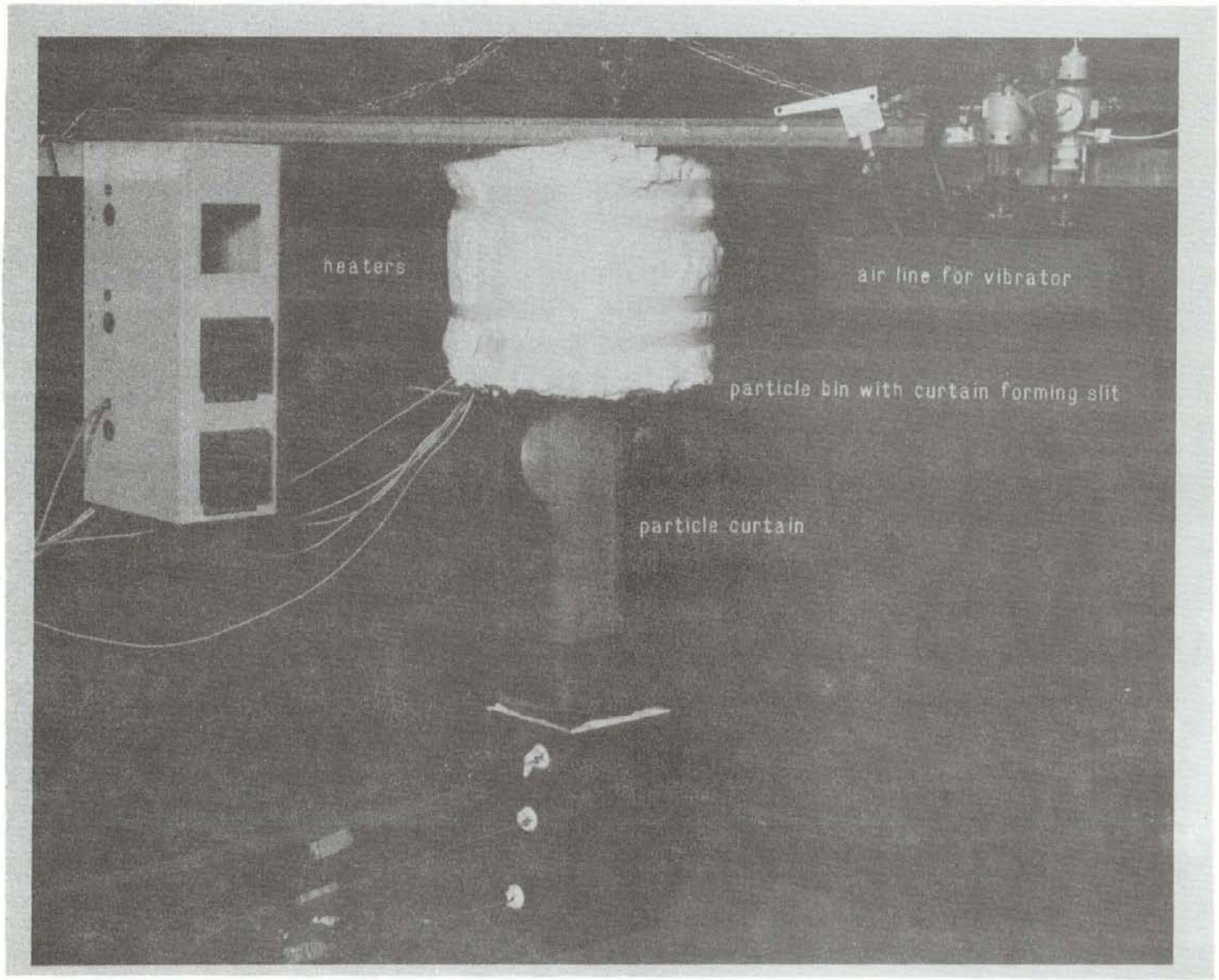

Figure 2. Photograph of experimental apparatus

techniques found useful in the laboratory tests will be applied to the full scale system hardware as the project proceeds. Therefore, the constraints imposed by the full scale system must be considered in the early stages of the subscale diagnostic development. Specifically, a device measuring particle velocity used on a full scale solid particle receiver will have to operate at least two meters away from the region of interest to insure that the instruments do not receive direct radiant flux or indirect radiation from heated surfaces. It must be capable of making measurements (1) on optically different types of particles, (2) in several directions, and (3) in a background of several hundred suns flux. Real time data acquisition is also needed so that measurements can be used to yield statistically valid data.

2. FLOW FIELD CHARACTERIZATION TECHNIQUES

High Speed Movie Photography

For dense curtains (particles occupying more than one percent of the space in any given volume) high speed movie photography seemed adequate to determine particle velocities by visually tracking a textured feature on the surface of the curtain. This technique is cumbersome because strong lighting, special high speed cameras and stop action projectors are required to analyze and determine the distance that the textured feature moves in a given length of time. Once the curtain is filmed (with a length scale in the field of view), the processed film must be viewed, a frame at a time, while a textured feature on the surface of the curtain is followed. By counting the number of frames viewed and using the photographed length scale to measure the total distance traveled, the average particle velocity on the curtain surface can be inferred, but not without much tedium. The accuracy of velocity measurement using this technique is subjective and depends on the observer's ability to track the textured feature on the curtain. Very early in this investigation, it was determined that curtains of this density were not suited for a particle receiver, and

hence no effort was made to verify whether or not curtain surface texture movement could be related to particle velocity. Consequently, this technique was not further pursued.

Flash Photography

In the particle ensembles of interest to the solid particle receiver program, the particle volume fraction is less than 0.1 percent. For this case, movie photography was not acceptable since there were no discernible textured features on the surface of the curtain that could be tracked. Attempts were made to introduce a band of colored sand into the curtain; however, after a meter of fall the band was so well mixed that it could not be distinguished. Therefore, a simple flash photography technique to measure particle velocity was developed. A standard electronic flash was instrumented with a photodiode and connected to a digital (Nicolet) storage oscilloscope. A 35 mm single lens reflex camera with a telephoto lens was focused on a length scale that resided in the curtain. When the shutter was triggered, the electronic flash discharged and the storage oscilloscope recorded the output signal (voltage) from the photodiode with one microsecond resolution. At first it was erroneously assumed that the stored photodiode trace was a true representation of the flash duration, but later tests revealed that the photodiode was being saturated. As a result the oscilloscope recorded a charge for about 200 microseconds longer than the actual duration of the flash. By placing neutral density filters between the flash and the photodiode, the saturation was eliminated and true flash durations were recorded (approximately 800 microseconds).

The particles appeared as streaks on the processed film. Those streaks that were clearly the result of a single particle's motion, appeared to be in focus with the scale in the photograph, and were in a region of realistic particle volume fraction were measured. In theory, the photographic streak length should be equal to the particle travel plus one particle diameter during a flash duration. However, the first half diameter of travel and the last half diameter of travel of the particle were

poorly illuminated because light was reflected for only a half diameter. The result was that the streak length visible on the photograph was indeed the distance of travel projected onto the image plane of the photograph.

This technique appears to be acceptable for individual particles but there is a strong tendency to select particles that may not be representative of the entire ensemble. For example, a statistical sampling based on this technique will give velocities somewhat lower than the average particle velocity because isolated particles are easier to measure, but probably travel more slowly than particles in a cluster. As with the movie photography technique, this method is also tedious and does not provide information in real time. Therefore, this technique may not work well in a dense curtain.

Tracer Particles

Some researchers [4,5] have used tracer particles to measure velocities in two phase flows. Typically these applications use detectors relatively close to the tracers. The tracing can be radioactive, fluorescent, magnetic, metallic, or simply optically different. In some cases, radio "pills" were used [6]. Because of the particle sizes of interest and distances over which measurements must be made, this method was not explored further.

Optical Correlation

Several papers [7,8] have described optical correlation techniques to measure the velocity of particles. The more common method employs two dual element fiber optic probes inserted into the flow field. Each probe has one element to direct light into the particle gas flow field. As a particle passes near the probe, some of the light is reflected into the other fiberoptic element for photodetection. As a group of particles passes by the first probe, it produces a very specific "fingerprint" on the photodetector, which is based on the relative arrival times of the particles. By

correlating these "fingerprints" or characteristic signals from the two probes, an average velocity of the particles can be calculated. One of the drawbacks of this technique is the requirement for the probe to be inserted into the flow field. For tests involving significant radiant flux, the probe would have to be cooled. For turbulent flow, these correlations become difficult. For these reasons this technique was also not explored further.

Laser Doppler Velocimetry

Laser Doppler velocimetry is used extensively to estimate the velocity of fluids or gases by seeding the fluid with small particles and inferring the velocity of the fluid by measuring the velocity of the particles. For this particular application, the particle velocity itself is of primary interest. The particles of concern in this study are much larger than usually used in gaseous LDV and present situations that are different from those reported in the literature. However, the advantages of laser Doppler velocimetry (LDV) implied that it should be evaluated for use in measuring particle velocity.

3. LASER DOPPLER VELOCIMETRY

Introduction

LDV is a method of measuring the velocity of moving objects by detecting the Doppler shift of light scattered by the objects. In order to produce and detect the Doppler shift for LDV measurements, optical components (typically a laser, lenses and a photodetector) must be employed in an appropriate arrangement. Although there have been many different optical arrangements designed to optimize the signal obtainable for particular fluid flow situations, there are two basic optical configurations commonly employed to measure the optical Doppler shift in LDV

measurements: the reference beam system and the real fringe or dual beam system.

An example of the reference beam system is shown in Figure 3. The output of the laser is split into two beams, a reference beam and an illuminating beam. The illuminating beam is directed at the flow region of interest where the moving object scatters light as it intersects the beam. The scattered light from the illuminating beam contains a Doppler shift proportional to the velocity of the moving object. This scattered light is photomixed, or heterodyned, with the unshifted light from the reference beam. For optimum signal to noise ratio, the reference beam needs to be attenuated prior to heterodyne mixing with the photodetector. This photomixing enables the Doppler shift to be detected by generating the difference frequency between the shifted and unshifted light. The difference frequency is lower than the frequency of the two light beams, and detection is therefore easier. The velocity can be calculated directly knowing this difference frequency and certain geometric

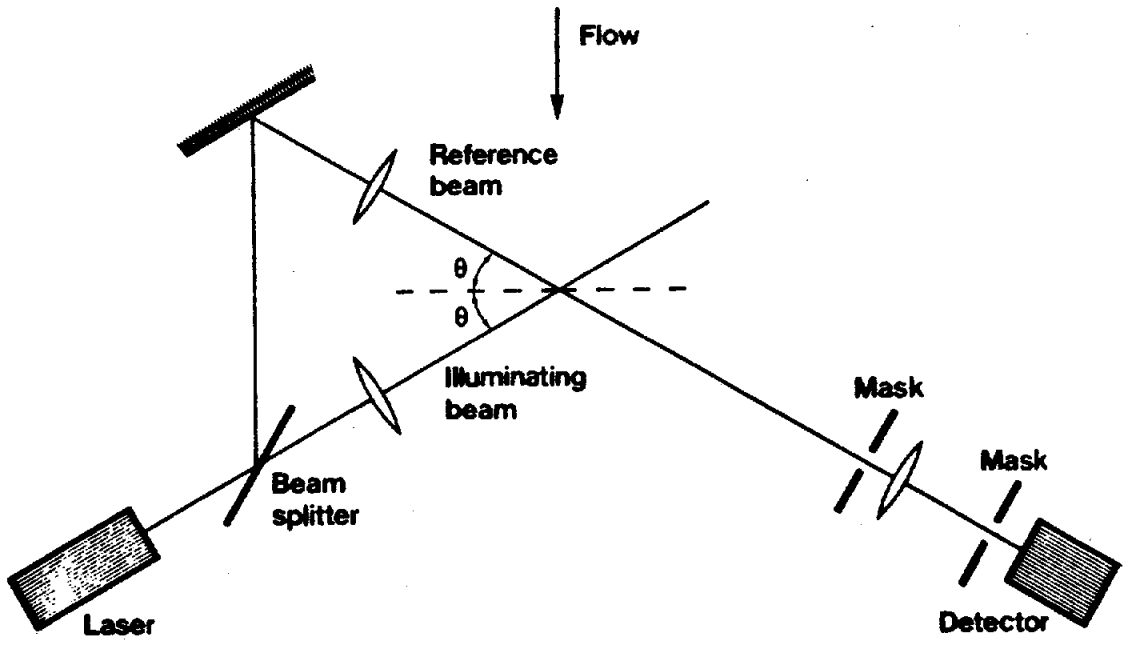

Figure 3. Schematic representation of a reference beam LDV system

parameters. Alignment needed for the reference beam optics, transmitting beam optics, and collection optics makes this system difficult to use in practice.

A real fringe system is shown in Figure 4. The real fringe system employs a single set of transmitting and receiving optics. As the beam leaves the laser it is split into two separate beams which are directed through the same optics equidistant from the optical axis. A final positive lens focuses the beams to intersect in the region of interest to form alternating bright and dark fringes by constructive and destructive interference. These fringes are then imaged onto a photodetector. Any object moving through the fringes scatters light as it passes each bright fringe. This scattered light produces a signal which has a frequency directly proportional to the rate at which the moving object crosses the fringe pattern. The photodetector for this system can be positioned at many different locations; the one shown in Figure 4 is for backscatter collection sharing the same transmitting optics. The

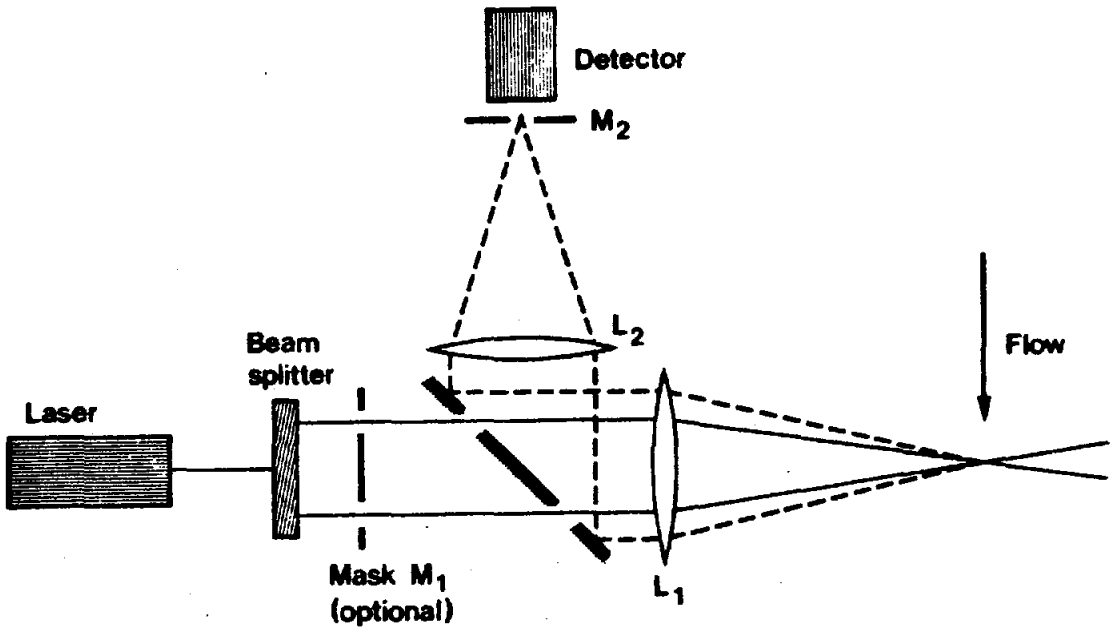

Figure 4. Schematic representation of a real fringe system

receiving optics can be placed in the forward direction or at any angle relative to the transmitting optics. The location of the receiving optics is a matter of optimization and practicality in each individual case. The backscatter configuration has the particular advantage of needing only one set of optics. Generally, the real fringe system is simpler to use in practice than the reference beam system because there are fewer optical components to align.

A closer look at the beam intersection aids in understanding the real fringe system. Figure 5 is an illustration of the fringe pattern created in space. The two planar wavefronts that are formed near the focal node of the objective lens constructively and destructively interfere to form alternating bright and dark fringes in space. When a particle passes through the fringe system it scatters light from the "bright" fringes and the velocity of the particle can be related to the rate of crossing the fringes. The velocity of the moving object is equal to the frequency of

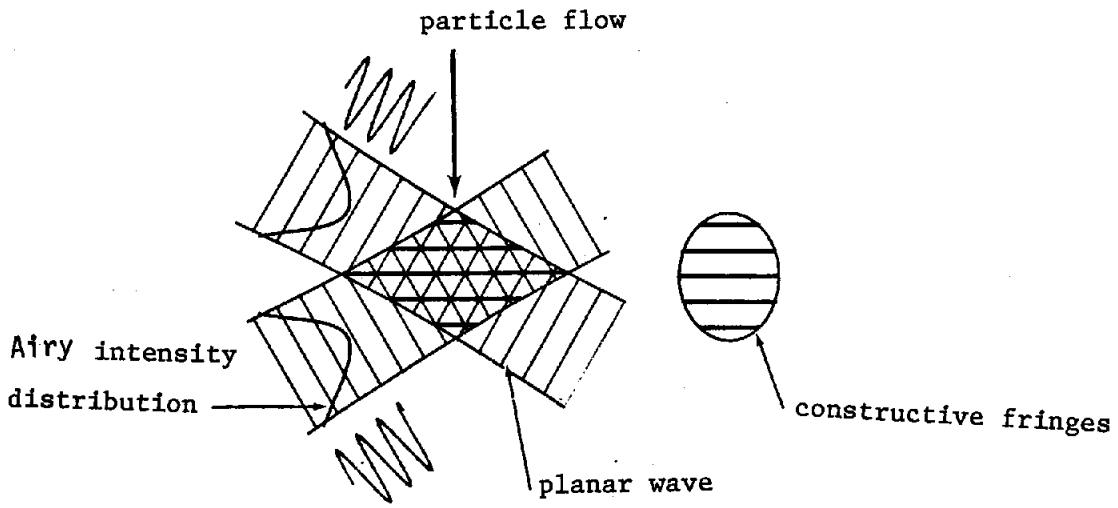

Figure 5. Representation of an LDV constructive interference fringe pattern at the focal node of a dual beam real fringe system

the detected signal multiplied by the fringe spacing. Because the two planar waves produced at the focal node of a simple positive lens have an Airy [17] intensity distribution, so does the interference pattern. This interference region or probe volume has an elliptic shape which is determined by the beam width and interference angle of the beams.

An ideal Doppler signal as detected by the photomultiplier viewing a real fringe LDV probe volume is shown in Figure 6. There are two amplitude modulations which characterize this signal, a pedestal or incoherent modulation and a fringe modulation. The pedestal signal is generally lower than the fringe signal and is caused by the incoherent scattering variation in intensity of the bright fringes brought about by the Airy nature of the intersecting laser beams. This pedestal signal would be produced if an incoherent light source were used to establish the dual beam configuration. The fringe signal is generally higher frequency than the pedestal signal and is created as a particle passes through the constructive interference fringe pattern. These signals are illustrated in Figure 6. The ratio of the magnitude of the Doppler frequency to pedestal signal defines visibility or signal strength.

If a particle larger than the fringe spacing passes through the fringes, a less modulated signal results, Figure 7. The rate of modulation in this case is less distinct because there is light scattered at all times from the bright fringes. Although increasing particle size increases the amount of scattered light received by the detector, the depth of modulation in light intensity is less. The classic visibility (ratio of the amplitude of Doppler sine wave to pedestal) curve shown in Figure 8 presents visibility as a function of the ratio of particle diameter to fringe spacing [12]. This visibility curve can be calculated using Mie theory for particles larger than the wavelength of light assuming light collection in the forward direction. It is apparent from this curve that a particle diameter to fringe spacing less than 2.2 is desirable for strong signals.

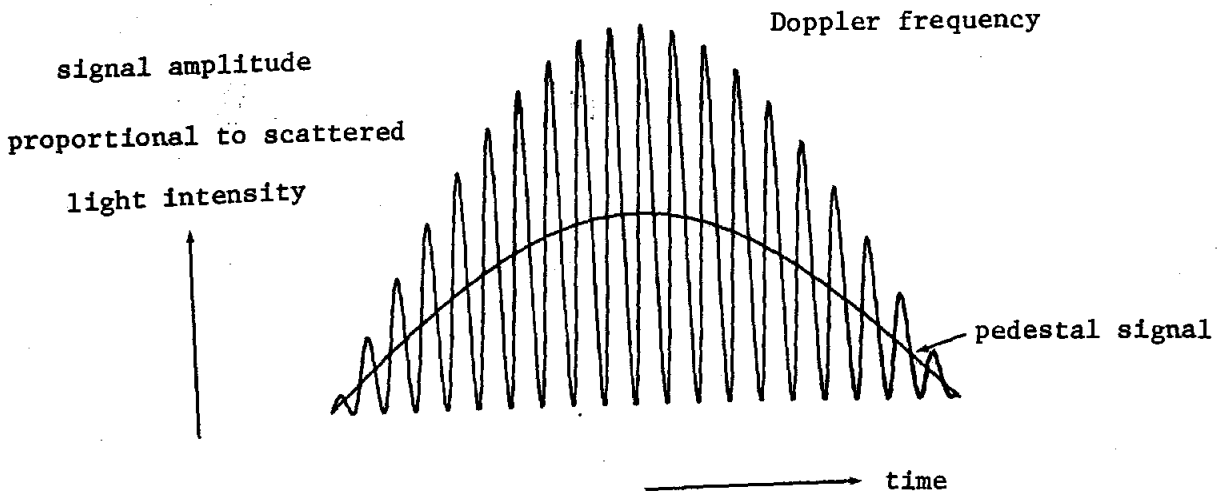

Figure 6. Representation of an ideal Doppler signal

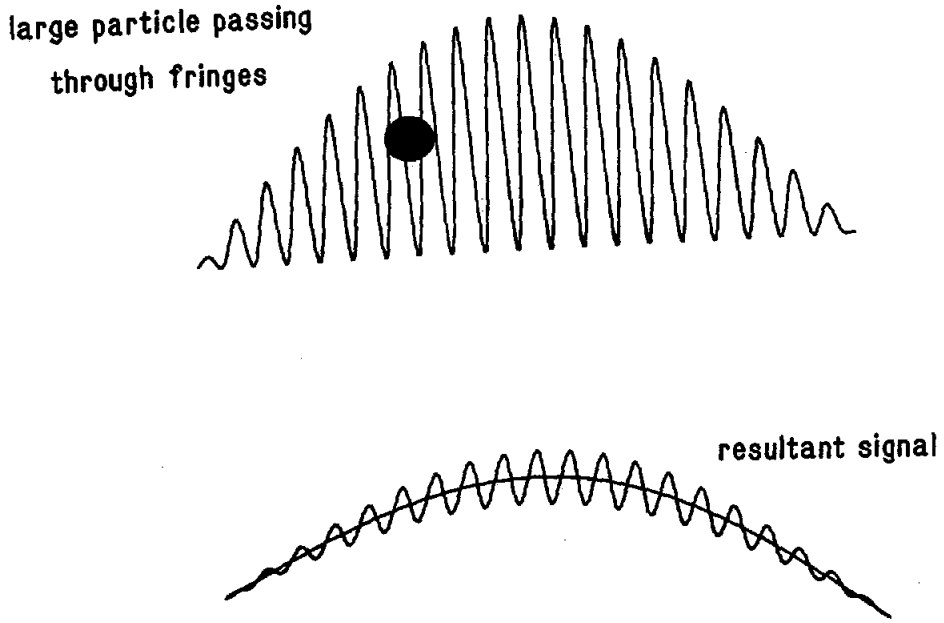

Figure 7. Representation of a less modulated Doppler signal

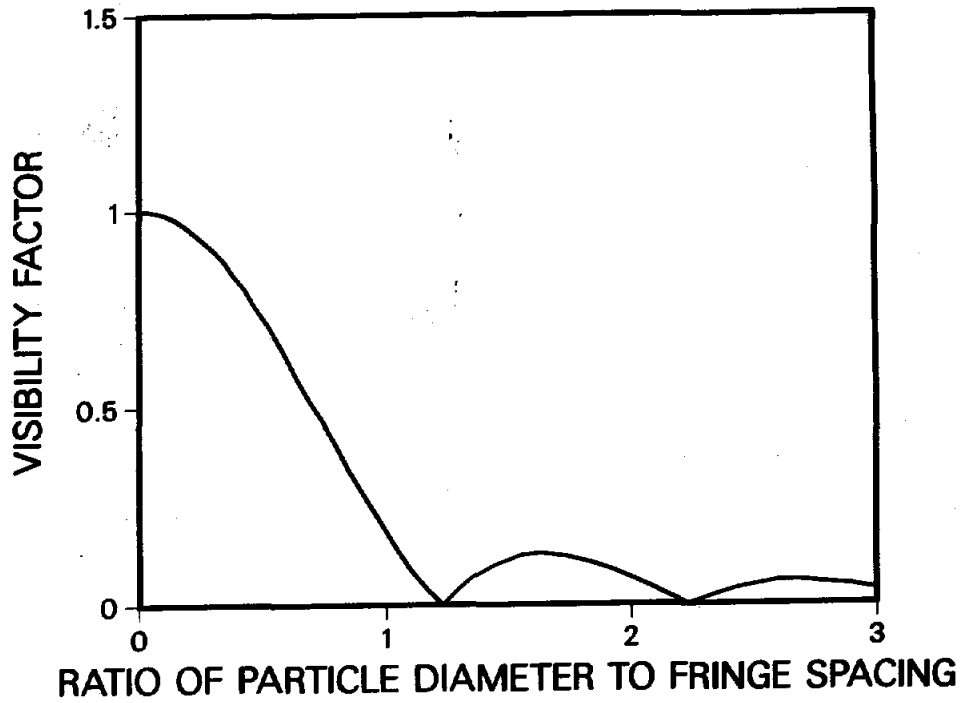

Figure 8. Classic visibility function

A typical frequency spectrum of the photomultiplier signal is shown in Figure 9. There is a low pedestal signal and a higher fringe scattering signal. In order to limit analysis to the fringe scattering signal, a high pass filter is used to reject the pedestal frequency. A low pass filter is also commonly employed to limit any noise that may be present at higher frequencies. Once the photomultiplier signal is conditioned, a symmetric Doppler burst results. The classic Doppler burst is shown in Figure 10.

Unfortunately, additional complications to signal processing are added as a result of noise. Noise is introduced into the system by particles outside the probe volume scattering light, inherent photomultiplier noise, and other light sources including room lights and reflected laser light from the walls or optical components. More important than the noise itself, however, is the signal to noise ratio (SNR). The basic equation for the SNR is given by

$$\frac{Power\ in\ Signal}{Power\ in\ Noise} = SNR \sim \left[\frac{a}{f}\right]^2 GV^2$$

where:

a = Particle diameter

f = Focal length of transmitted beams

G = Scattering parameter (non-dimensional scattering function)

V = Visibility parameter (non-dimensional measure of the depth of modulation in fringe scattered signal)

Consideration of these parameters for SNR optimization is necessary. Large particles and long focal lengths are required in this particular application of LDV. These two requirements have competing effects on the SNR. The particle size for this application could not be altered for SNR optimization because it was a parameter of major importance in the solid particle receiver. Because SNR increases as the focal length decreases, the focal length should be the minimum necessary to meet system constraints. In this case a focal length of two meters was considered the minimum acceptable for full scale solid particle receiver application. The scattering

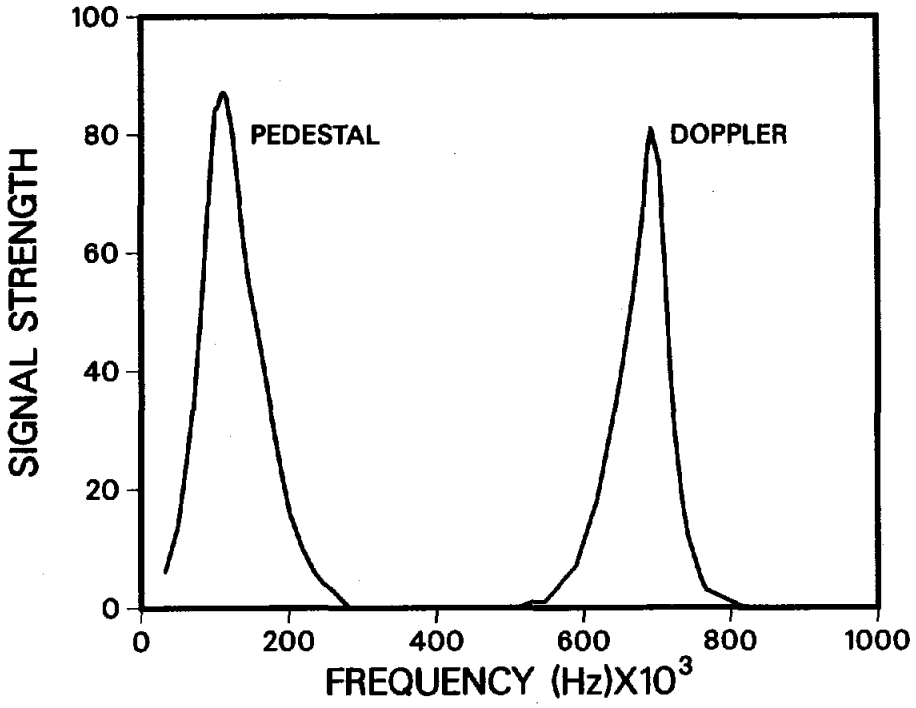

Figure 9. Frequency spectrum of photomultiplier signal. Fourier transform of photodetector signal showing the incoherent pedestal and coherent Doppler signals.

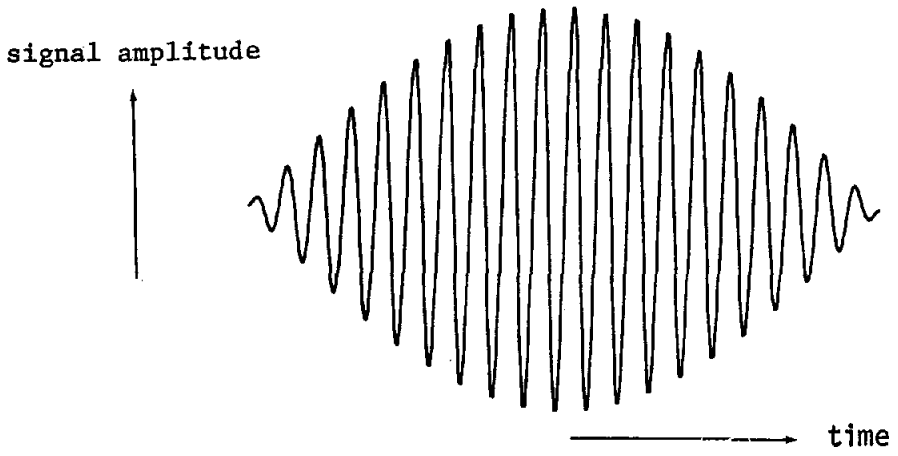

Figure 10. Classic Doppler burst after original conditioning rejects low frequency incoherent signal and high frequency plasma noise from the laser.

parameter, G, is a function of angle, and therefore the location of the collection optics can be chosen to obtain the best SNR for any given particle if the scattering characteristics are known or can be calculated. The SNR increases as the visibility parameter squared, V^2, thereby making high visibility a valuable parameter for SNR optimization. Care should be taken to choose an appropriate particle diameter to fringe spacing ratio to obtain high visibility.

Determining Particle Velocities in Two Phase Flow

Measuring the velocities of large particles falling in a curtain is a unique application of LDV. The uniqueness arises because of the application, requirements, and particle characteristics involved. As mentioned earlier, the usual application of LDV is for measurement of fluid velocities where the fluid flow is seeded with small spheres that are assumed to move at the fluid velocity. However, the present case is

unique because the velocities of the particles themselves are desired (regardless of the surrounding gas velocity). In addition, some of the tests will require that velocities be measured at depths of one meter into the particle curtain with particle volume fractions approaching 0.1 percent. The particles of interest here are also large compared to the particles used for seeding fluid flows. Typical particle diameters are 10 to 100 times larger, and are not spherical. Particle materials of interest include sand, silicon carbide, rutile, and other ceramics such as Al_2O_3 and master beads.

A. Preliminary LDV Experiment

A preliminary LDV experiment to measure the velocity of sand particles was conducted to obtain an estimate for signal strength and SNR in such a system. The system employed had a fringe spacing of 4.76 microns (particle diameter/fringe spacing ratio of 60, particle diameter/probe volume ratio of 3). The focal length was 762 mm and a 3.75 times beam expander and the backscatter collection mode was used.

The results of the preliminary experiment proved that LDV could be used in clouds of sand. However, the signals obtained from the photomultiplier were noisy and a had low SNR due to the very large particle diameter to fringe spacing ratio. Since reasonable velocity measurements were obtained and since the laser had no trouble penetrating the particle curtain, it was decided to extend the measurements to encompass the conditions imposed by a real system.

B. Refined Experimental System

The results obtained from the preliminary experiment were encouraging and a new LDV arrangement was designed to help improve the SNR and have a capability of making full scale field measurements, i.e. making velocity measurements at distances greater than two meters. The fringe spacing was expanded to 21.6 microns

(particle diameter/fringe spacing ratio of 15, particle diameter/probe volume ratio of 0.3). A focal length of 2.2 m was used without a beam expander and with both on-axis and off-axis collection to examine the effects on SNR. A laser line filter was installed in the photomultiplier to eliminate light from other sources. A photograph of the system optics and laser is shown in Figure 11.

On-axis and off-axis collection produced nearly identical results. This is believed to be due to the non-spherical and rough nature of the particles. The signal strength was good, and a satisfactory SNR was obtained using back scatter and no beam expansion. The results with this system were encouraging. Velocity measurements could be made with minimal optics.

C. Reasons for Success

Results of the refined LDV system illustrated that accurate velocity measurements could be made with a simple optical arrangement. This was unexpected because SNR estimations indicated that a more complex optical system was necessary. However, the complexities involved in calculating the scattering parameter and visibility parameter for the particles involved in this application make estimation of SNR difficult at best.

The irregular shape and reflecting facets of the sand, silicon carbide and rutile particles tested thus far make the scattering function impractical to calculate. Usually LDV is performed on small spherical particles, and the scattering function can be predicted by employing Mie theory. However, in this case the surface of the particles is non-spherical, rough, partially diffuse and partially specular.

The visibility (magnitude of Doppler frequency/magnitude of pedestal frequency) for the particles of interest is also difficult to predict. The classic visibility curve has been found to be accurate for large particles when light is collected in forward scatter [12]. However, in this experiment back scatter is employed. Visibility in back scatter is usually larger than visibility in forward scatter for large diameter to fringe spacing ratios [12]. Therefore, the classic visibility curve likely underpredicts

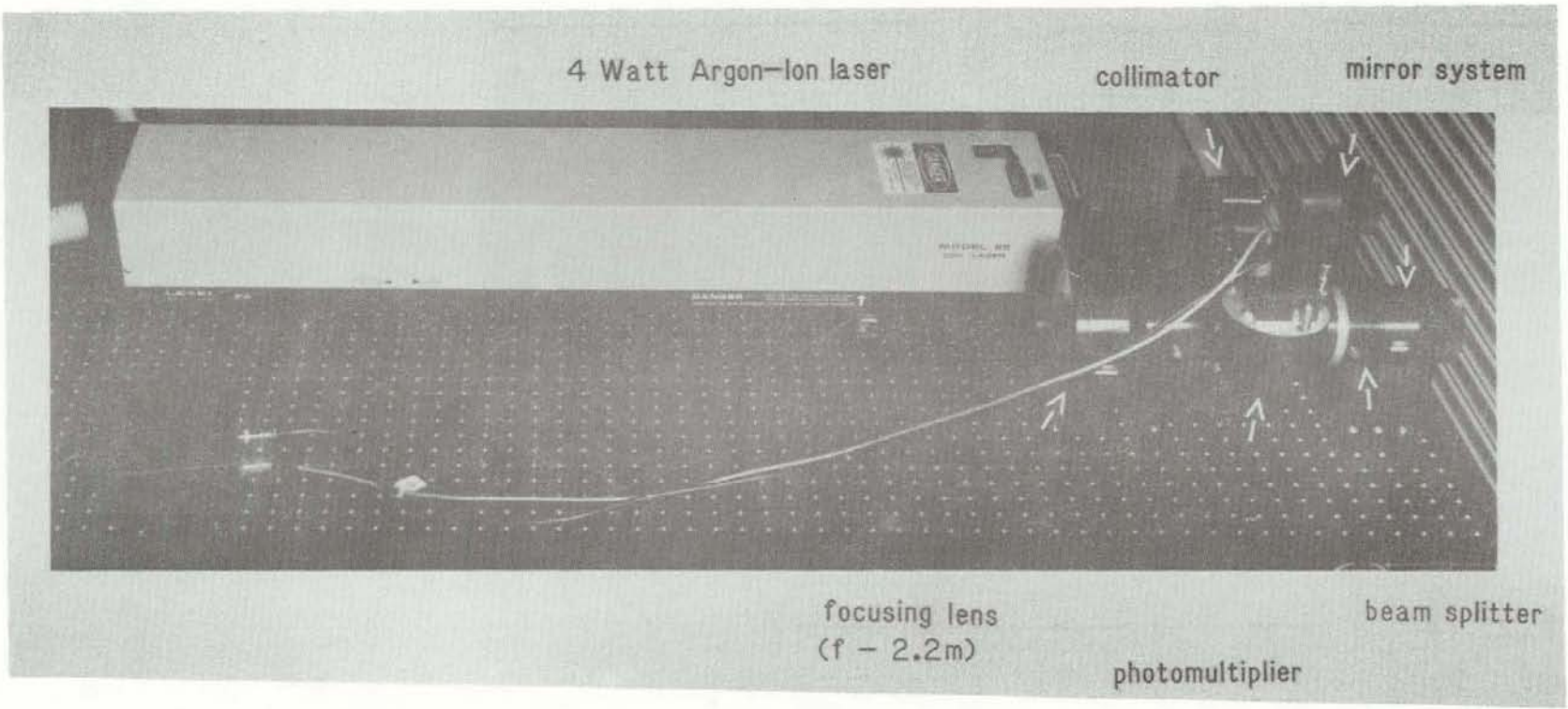

Figure 11. Photograph of LDV system optics

the visibility for this case. In addition, visibility has been found to be a function of particle size, shape, and refractive index as well as size, shape and location of the collection aperture on the photodetector. Figure 12 illustrates how the refractive index can be more important than the ratio of particle diameter to fringe spacing in determining visibility [9]. The concept of the visibility being greater than theoretically determined is verified for signals obtained with particle diameter to fringe spacing ratios of 15. Further discussions on the visibility function can be found in References 10 and 11.

Laser Doppler Velocimetry to Determine Particle Volume Fraction

Measuring particle volume fraction in a dense stream of falling particles was another aerodynamic parameter of interest in modeling solid particle receivers.

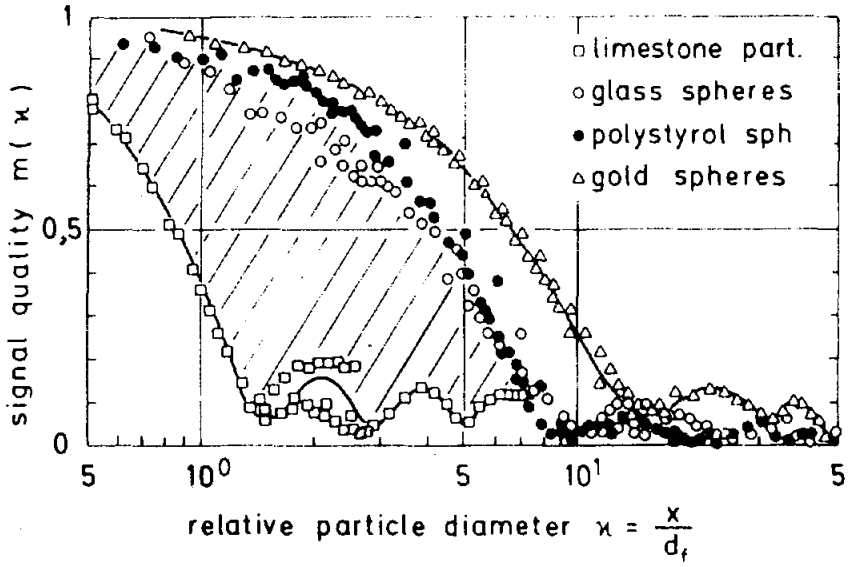

Figure 12. Visibility as a function of particle diameter (from Ref. 14)

After several experiments it was determined that this measurement was difficult using LDV. There are two major reasons for the difficulty.

One difficulty results from uncertainties in the dimensions of the probe volume. The probe volume is defined by the line width of the two intersecting beams. The width of a laser beam is commonly defined as the distance between those points having an intensity equal to $1/e^2$ of the the maximum intensity. This defines the line width as being the width between the 1/e power points. The exact line width is not known in general. Therefore, even if an accurate count of particles is obtained, the particle volume fraction calculation will contain some error due to the uncertainty in the probe volume.

Another difficulty in measuring volume fraction results from particles in the beams masking the probe volume. In order to obtain accurate volume fractions, a count of the particles in the control volume in real time must be obtained. When intervening particles mask the probe volume, real time acquisition is disturbed.

4. PARTICLE AND CURTAIN BEHAVIOR

Information concerning particle and curtain behavior in free-falling particle ensembles was obtained from three of the techniques discussed in this report: high speed movie photography, flash photography, and LDV. The velocity data obtained from each of these techniques is presented in this section. Qualitative discussion concerning flow field turbulence and curtain behavior is also included.

High Speed Movie Photography

This technique was used on two curtain geometries: 0.3 mm diameter sand flowing through a 6 mm by 150 mm slit, and 0.6 mm diameter sand flowing through 4.8 mm diameter holes arranged in hexagonal close pack geometry. The initial volume fraction in both of these cases exceeded ten percent. In Figure

13 the measured velocities are compared to velocities of particles falling with no air resistance (in a vacuum) with varying initial velocities. The data compares most favorably with particles having an initial velocity of 2 m/s. The apparent absence of aerodynamic drag is not surprising in view of the extremely dense curtain geometry and the proximity of the measurements to the curtain forming slit. Particle velocities in excess of 6 m/s after only two meters of fall would not provide sufficient residence time in a solid particle receiver to allow a significant absorption of the solar energy and subsequent tests were conducted using less dense curtains.

In the second test the measured velocities were compared to a theoretical approach to a specified terminal velocity and the results are shown in Figure 14. These data imply that the particles have not yet reached terminal velocity, which is greater than 7 m/s. The scatter in the data demonstrates the need for a more accurate measurement technique.

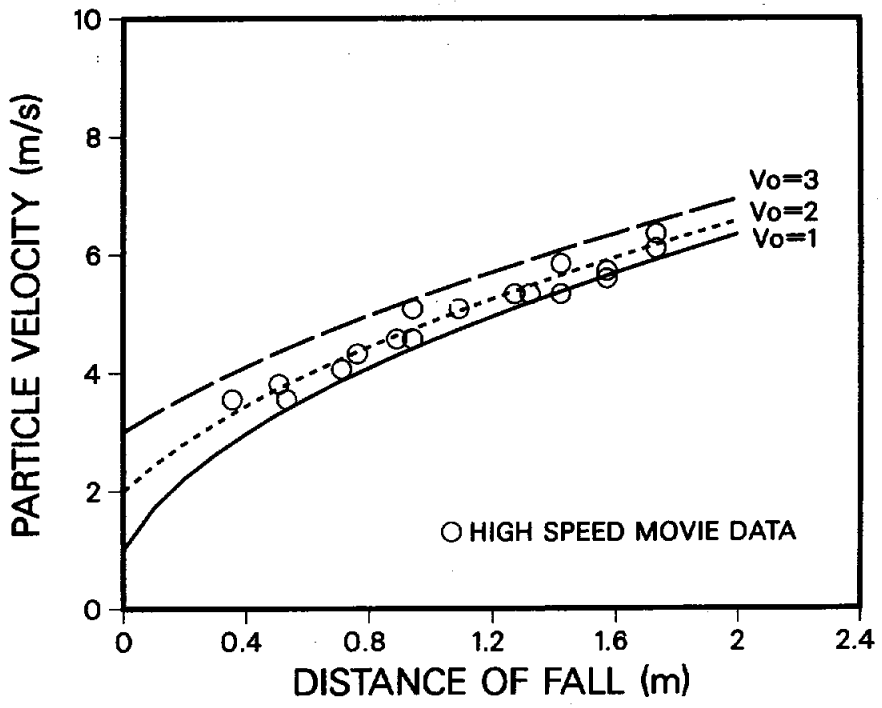

Figure 13. Velocity of 300 μm silica sand compared to free fall without aerodynamic drag

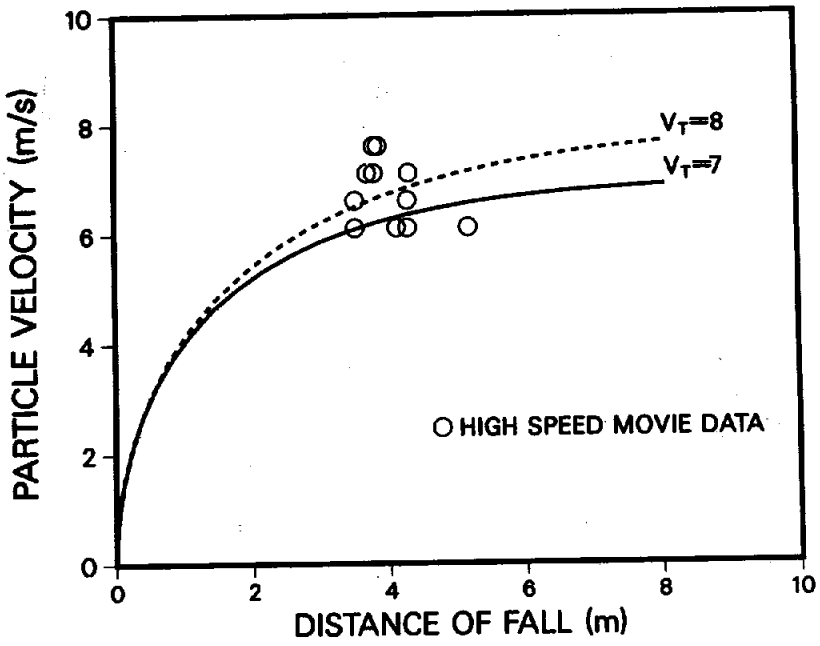

Figure 14. Velocity of 300 μm diameter silica sand compared to approach to a theoretically determined terminal velocity.

Flash Photography

A. Velocity Measurements

Figure 15 is a composite of several data sets made using flash photography. The flow conditions for each set were identical and provided comparative data for up to six meters of fall. To reduce the curtain density, a #12 mesh screen was used to cover the 6 mm slit. Not only did this screen disperse the curtain, it also reduced the initial velocity and the mass flow rate or mass flux. The large scatter in these data is not due entirely to measurement error but is believed to be an indication of velocity fluctuations that can occur. The measurement error associated with the data is illustrated by the error bar on the velocity measurement at a three meter fall distance in Figure 15. This error is primarily a result of the difficulty associated with

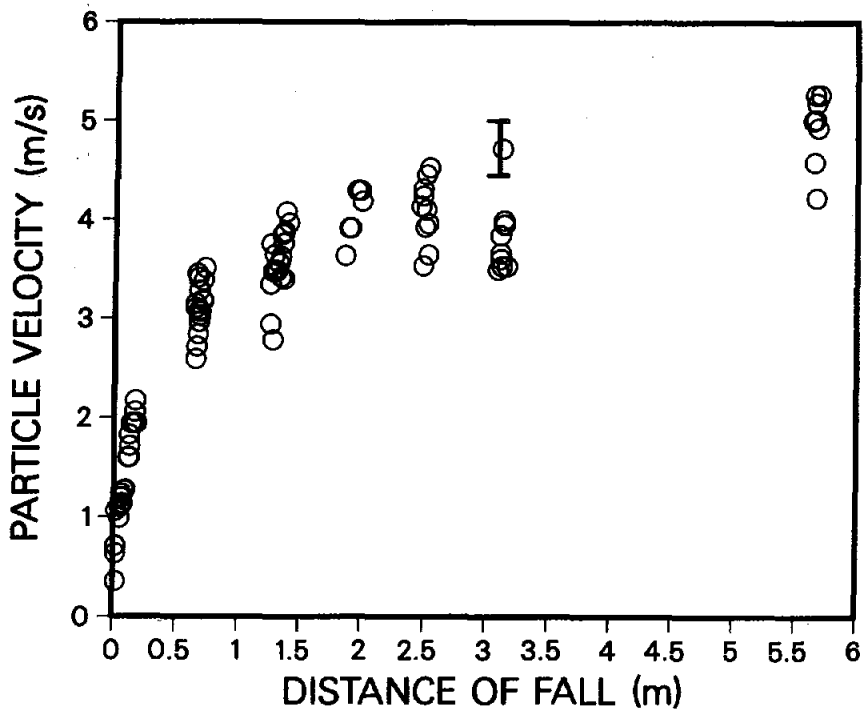

Figure 15. Velocity of 300 μm diameter silica sand as a function of distance of fall.

measuring the streak length accurately. Secondary reasons for the error are strobe timing accuracy (one microsecond resolution), and the particle being out of focus with the length scale in the photograph. With the velocity fluctuations indicated in Figure 15, the need for statistically meaningful data becomes readily apparent. If, for example, the streak selection from the photographs preferentially chooses the slower moving particles, these data can be significantly skewed since the technique permits only a small number of streaks to be measured at any one time. For a meaningful statistical sample, several hundred measurements per location would be needed. Such a sampling rate is impractical using photographic techniques.

B. Flow Field Turbulence

In addition to the velocity data, much information was gained on the particle velocity fluctuations. On a microscopic scale the particles do not exhibit any

turbulence as shown in the photographs of Figure 16. Greater than ninety nine percent of the particles are falling in parallel with the rest of the particles. Very few particles were seen colliding with other particles. No erratic particle motions were detected. On a macroscopic scale, the particle curtain was very stable up to approximately one meter of fall after which curtain position, shape and uniformity varied considerably. As the distance of fall and velocity increased, so did the instability (see photographs, Figure 17).

C. Curtain Geometry

The area of the curtain expands as the particles fall. Curtain thickness as a function of fall height is shown in Figure 18 for 0.6 mm diameter sand flowing through a 6 mm thick by 150 mm wide slit. Again the curtain is stable until about one meter of fall, after which it becomes very unstable and varies in thickness by as much as 300 percent as illustrated in Figure 18.

Laser Doppler Velocimetry

The velocities measured with LDV are superimposed on the photographic velocity data and are presented in Figure 19. Each LDV point is an average of 1000 or more recorded particle velocities. Because the particle flow field is not turbulent, the particle size is uniform, and the particle velocity rather than the gaseous velocity is desired, the chances of velocity bias are minimal. The measured velocity distributions were Gaussian, and the error associated with the mean velocity is assumed to be characterized by the standard deviation of the measurements, σ, and the number of measurements taken, N. The deviation of the mean velocity is therefore $\frac{\sigma}{\sqrt{N}}$. The resultant errors are $\pm$ 1.5 percent [15]. It is seen that there is good agreement between the velocities measured by the photographic technique and LDV although the flash photography velocities have a tendency to be slightly lower than the those recorded with LDV. This result is not surprising,

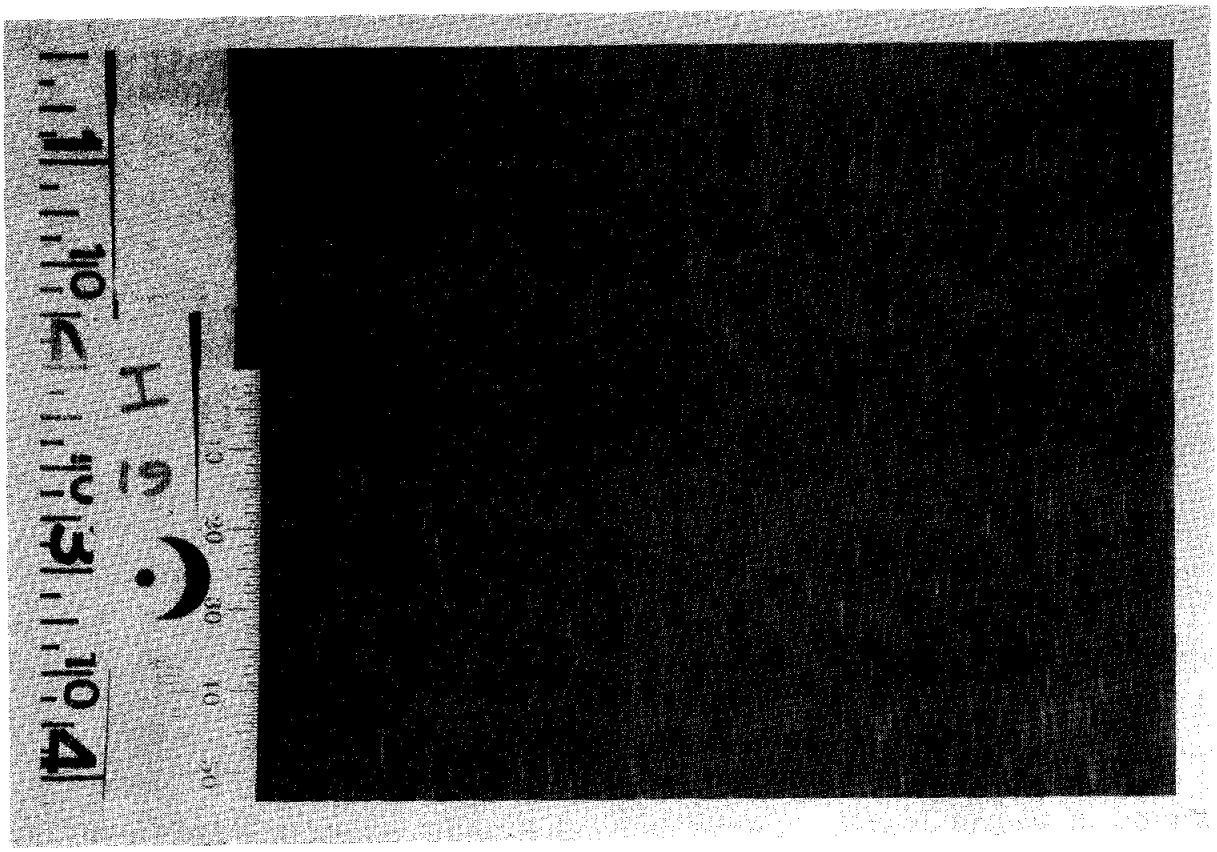

Figure 16. Photograph of particle curtain demonstrating the absence of turbulence

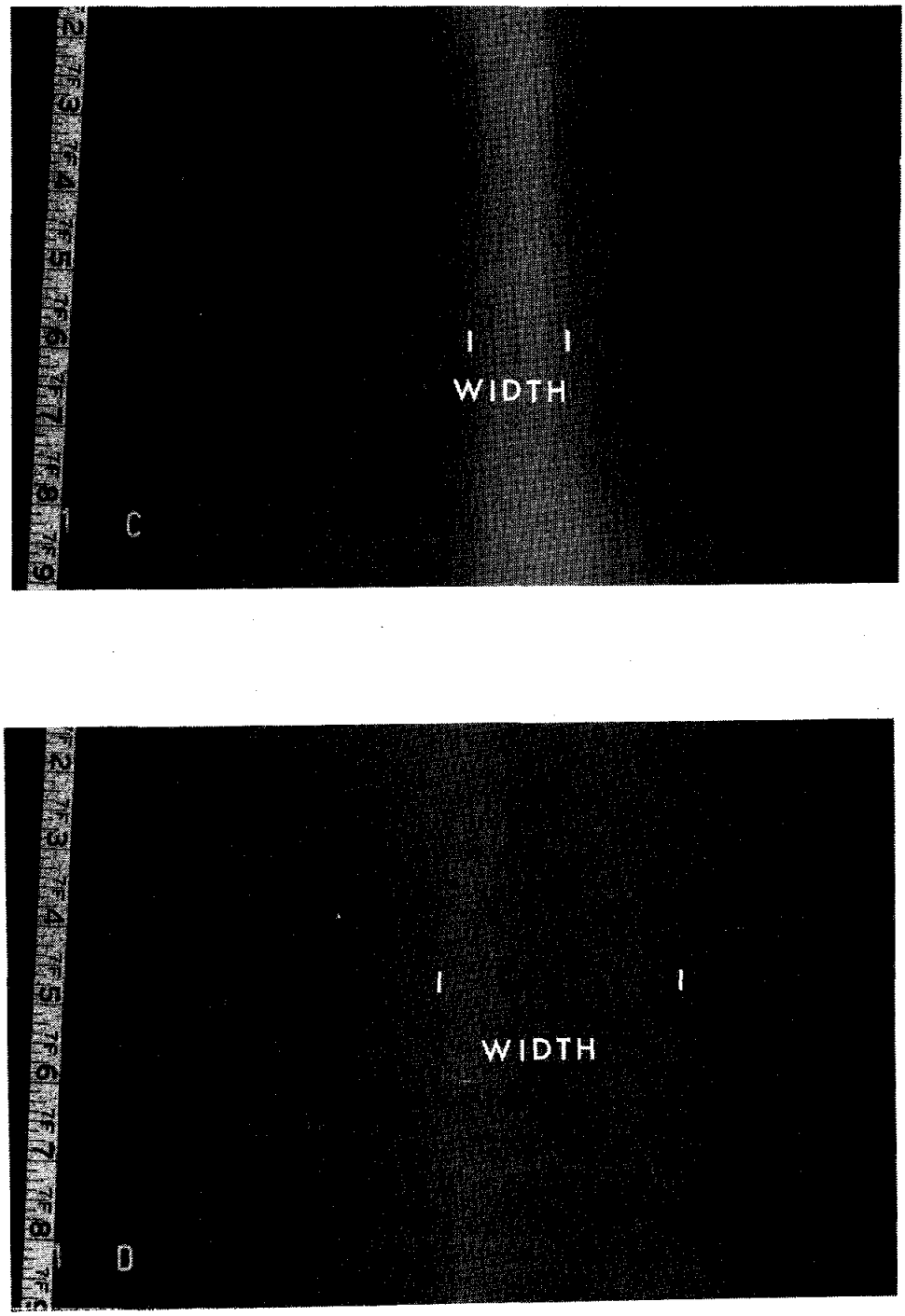

Figure 17. Photograph of particle curtain demonstrating macroscopic instability (Photographs made at different times)

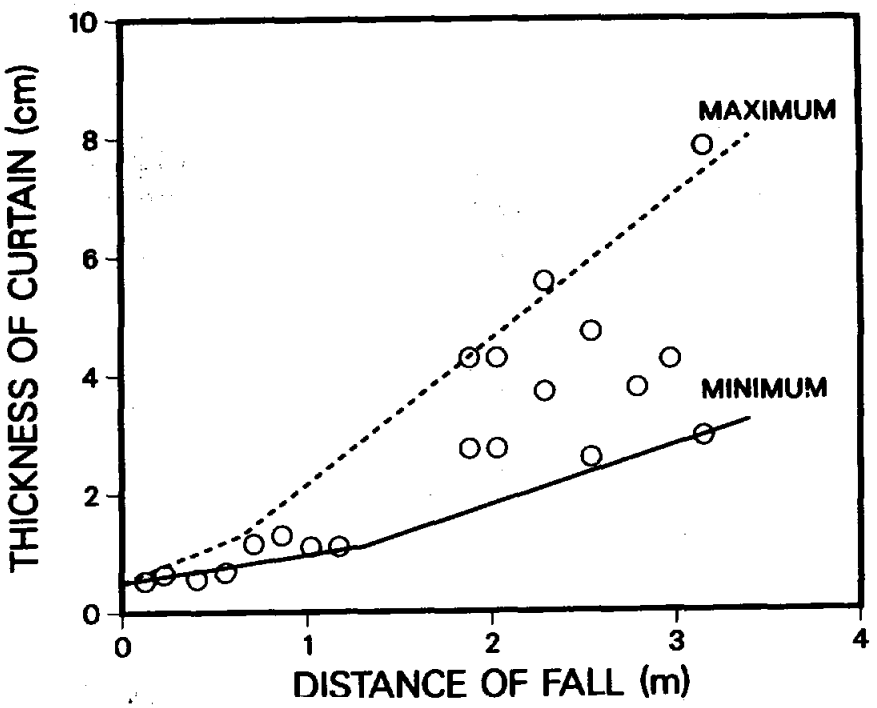

Figure 18. Particle curtain expansion as a function of distance of fall

since the photographic technique favors slow moving particles (well-defined streaks).

Discussion of Results

The measured particle velocity profile is compared with the theoretical velocity of a free-falling single isolated sphere (with the same effective diameter) in Figure 20. It is seen that the particle velocity in the ensemble of particles is greater than the single isolated sphere velocity. This result can be explained if influx of ambient air into the curtain is considered. However, if the particles were confined in a manner which allowed no influx of air, the trend would be reversed. This phenomena is best understood by examining the drag coefficient and drag force in two-phase flows.

The drag coefficient for gas-particle two-phase flows has been determined and is greater than that for a single sphere in free fall [13, 16]. This implies that in two-phase flows where the gas velocity is nearly zero, the solid particle velocity in an

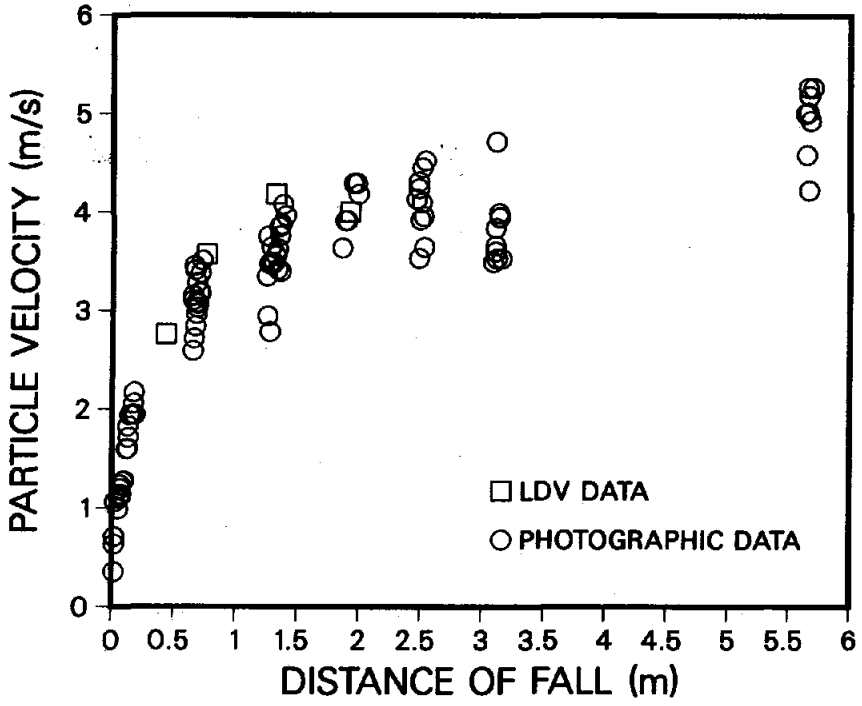

Figure 19. Comparison of velocity measurements from LDV and flash photography techniques

ensemble of particles is less than the velocity of a single isolated sphere because the drag coefficient (and force) is higher. Two-phase pipe flow is an example where the ensemble particle velocity is lower than the theoretical velocity of a single isolated sphere in free-fall.

However, when the gas velocity in two-phase flow is significant, particle ensemble velocities can be larger than single isolated sphere velocity. If the gas velocity is high enough, it offsets any increase in drag coefficient. Recall the definition of drag force,

$$F_D = \frac{1}{2}\rho C_D(v_s - v_g)|v_s - v_g|$$

where:

F_D = Drag Force

C_D = Drag Coefficient

ρ = Gas Density

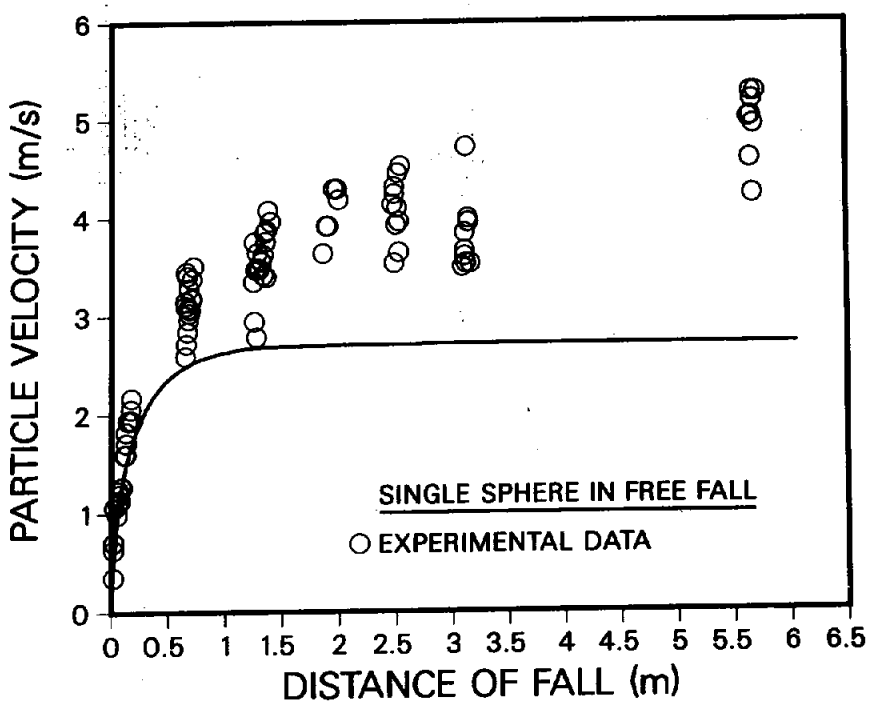

Figure 20. Comparison of experimental data and single sphere velocities

v_s = Solid Velocity
v_g = Gas Velocity

Therefore, as the velocity of the gas approaches the velocity of the solid, the drag force decreases. This decrease in drag force would result in an increase in particle velocity. The particle velocity can therefore be greater than single isolated sphere velocity. The limit of this example is when the gas velocity and particle velocity are equal which results in a flow which behaves like free-fall without air resistance (in a vacuum).

5. CONCLUSION

After evaluating many techniques to measure particle velocity in ensembles of falling particles, a laser Doppler velocimetry system was developed. The application

of LDV to measure particle velocities in the two-phase flows of interest to the solid particle receiver program was unique, and successful measurements were completed. The results of the LDV measurements agree with results using flash photography. A comparison of the measured particle velocity for the two techniques is shown in Figure 19.

Two-phase particle velocities in particle ensembles are greater than the velocity of a free-falling single isolated sphere of the same effective diameter. This is believed to be due to the influx of air into the particle stream. Particle-particle interactions in developed flow are negligible, and there is curtain instability after one meter of fall.

REFERENCES

1. J. Martin and J. Vitko, Jr., "ASCUAS: A Solar Central Receiver Utilizing a Solid Thermal Carrier," Sandia National Laboratories, SAND82-8203, 1982.

2. P. K. Falcone, J. E. Noring, and C. E. Hackett, *Proceedings of the 17th Intersociety Energy Conversion Engineering Conference,* Vol. 3, 1982, pp. 1498-1503.

3. R. Clift, J. R. Grace and M. E. Weber, *Bubbles, Drops and Particles,* N. Y. Academic Press, 1978.

4. N. B. Kondukov et al., "An investigation of the parameters of moving particles in a fluidized bed by a radioisotopic method," Int. Chem. Eng., Vol. 4, 1964, p. 43.

5. D. VanVelzen, H. J. Flamm, H. Langenkamp and A. Casile, "Motion of solids in spouted beds," Can. J. Chem. Eng., Vol. 52, 1974, p. 156.

6. M. F. Handley and M. G. Perry, Rheol. Acta, Vol. 4, 1965, p. 225.

7. Katsuya Oki, Takashi Akehata and Takashi Shirai, "A new method for evaluating the size of moving particles with a fiber optic probe," Powder Technology, Vol. 11, 1975, pp. 51-57.

8. Katsuya Oki, Walter P. Wallawender and Liang-Tseng Fan, "An inexpensive and simple correlator for velocity measurements," Ind. Eng. Chem. Fundam., Vol. 17, No. 4, 1978.

9. Franz Durst, "REVIEW- Combined measurements of particle velocities, size distributions, and concentrations," Transactions of the ASME, Vol. 104, September 1982, p. 284.

10. William D. Bachalo, "Method for measuring the size and velocity of spheres by dual-beam light scatter interferometry," Applied Optics, Vol. 19, No. 3, February 1, 1980, p. 363.

11. L. E. Drain, *The Laser Doppler Technique*, John Wiley and Son Ltd., 1980, p. 197.

12. Ronald J. Adrian, Kenneth L. Orloff, "Laser anemometer signals: visibility characteristics and application to particle sizing," Applied Optics, Vol. 16, No. 3, March 1977.

13. Sabri Ergun, "Fluid flow through packed columns," Chemical Engineering Progress, Vol. 48, No. 2, February 1952, p.89.

14. A. Stumke and H. Umhauer, "Local particle velocity distributions in two-phase flows measured by laser-Doppler velocimetry," Proceedings of the Dynamic Flow Conference, Marseille, France, 1978.

15. H. D. Young, *Statistical Treatment of Experimental Data*, McGraw Hill, 1962.

16. S. L. Soo, *Fluid Dynamics of Multiphase Systems*, Blaisdell Publishers, 1967, p. 188.

17. F. A. Jenkins and H. E. White, *Fundamentals of Optics*, McGraw Hill, Fourth Edition, 1976.

UNLIMITED RELEASE INITIAL DISTRIBUTION:

U.S. Department of Energy (4)
Forrestal Building, Room 5H021
Code CE-314
1000 Independence Avenue, S.W.
Washington, D.C. 20585
Attn: C. Carwile
H. Coleman
F. Morse
M. Scheve

U. S. Department of Energy (2)
P.O. Box 5400
Albuquerque, NM 87115
Attn: D. Graves
J. Weisiger

U.S. Department of Energy (4)
1333 Broadway
Oakland, CA 94612
Attn: T. Heenan
R. Hughey
G. Katz
W. Lambert

North Carolina State University
P.O. Box 7905
Chemical Engineering Department
Rayleigh, NC 27695
Attn: Prof. Ruben Carbonell

University of California
Department of Mechanical Engineering
6167 Etcheverry Hall
Berkeley, CA 94720
Attn: Prof. Ralph Greif

University of Houston
Solar Energy Laboratory
4800 Calhoun
Houston, TX 77704
Attn: A. F. Hildebrandt

Washington State University
Department of Mechanical Engineering
Pullman, WA 99164-2920
Attn: Prof. Clayton Crowe

Applied Aeroponics
7000 Village Parkway
Suite 1
Dublin, CA 94566
Attn: Victor P. Burolla

Centre National De La Recherche Scientifique (2)
Laboratorie d'Energetique Solaire
Odiello, B.P. 5, 66120 Font- Romeu
France
Attn: G. Flamant
C. Royere

Electric Power Research Institute (2)
P.O. Box 10412
Palo Alto, CA 94303
Attn: J. Bigger
E. DeMeo

Electro-Optic Systems Section
Pacific Northwest Laboratories
Battelle Boulevard
Richland, WA 99352
Attn: Dr. J. W. Griffin

Lawrence Berkeley Laboratories 90-2024
Berkeley, CA 94720
Attn: Dr. Arlon Hunt

Solar Energy Research Institute (2)
1617 Cole Boulevard
Golden, CO 80401
Attn: B. Gupta
R. Hulstram

Southern California Edison (2)
P. O. Box 800
Rosemead, CA 92807
Attn: J. N. Reeves
P. Skvarna

R. B. Pettit, 1824
F. P. Gerstle, 1845
J. R. Hellmann, 1845
T. A. Michalske, 1845
E. H. Beckner, 6000; Attn: V. Dugan, 6200
D. G. Schueler, 6220
J. V. Otts, 6222
P. L. Class, 7531

R. S. Claassen, 8000; Attn: D. M. Olson, 8100
A. N. Blackwell, 8200
D. L. Hartley, 8300

C. S. Selvage, 8000A

C. W. Robinson, 8240; Attn: G. A. Benedetti, 8241
M. L. Callabresi, 8242
M. R. Birnbaum, 8243

C. E. Hackett, 8244
C. M. Hartwig, 8244
W. G. Houf, 8244
G. H. Evans, 8245

M. E. John, 8245
C. A. LaJeunesse, 8245
C. S. Hoyle, 8249

R. C. Wayne, 8400; Attn: L. D. Bertholf, 8430
H. Hanser, 8440
R. L. Rinne, 8470

J. B. Wright, 8450
A. C. Skinrood, 8452
P. K. Falcone, 8453
J. M. Hruby, 8453 (10)
G. H. Prescott, 8453
B. R. Steele, 8453
J. C. Swearengen, 8453
J. B. Wright, 8454 (actg.)
Publications Division, 8265, for TIC (27)
Publications Division, 8265/Technical Library Processes Division, 3141
Technical Library Processes Division, 3141 (3)
M. A. Pound, 8024, for Central Technical Files (3)